PERGAMON

International Journal of Solids and Structures 40 (2003) 3477–3492

INTERNATIONAL JOURNAL OF SOLIDS and STRUCTURES

www.elsevier.com/locate/ijsolstr

Approximate dynamic boundary conditions for a thin piezoelectric layer

Gunnar Johansson, A. Jonas Niklasson *

Department of Applied Mechanics, Chalmers University of Technology, SE-412 96 Göteborg, Sweden

Received 5 July 2002; received in revised form 14 February 2003

Abstract

Approximate dynamic boundary conditions of different orders are derived for the case of a thin piezoelectric coating layer bonded to an elastic material. The approximate boundary conditions are derived using series expansions of the elastic displacements and the electric potential in the thickness coordinate of the layer. All the expansion functions are then eliminated with the aid of the equations of motion and boundary/interface conditions of the layer. This results in boundary conditions on the elastic material that may be truncated to different orders in the thickness of the layer to obtain approximate boundary conditions. The approximate boundary conditions may be used as a replacement for the piezoelectric layer and thus simplify the analysis significantly. Numerical examples show that the approximate boundary conditions give good results for low frequencies and/or thin piezoelectric layers.

Keywords: Approximate boundary condition; Piezoelectric; Thin coating; Sensor; Actuator; Elastodynamic

1. Introduction

In this paper, our attention is focused on the approximation of *thin* piezoelectric layers perfectly bonded to elastic non-piezoelectric materials. Piezoelectric materials are commonly used in actuators and/or sensors in a number of applications. Traditional applications are, for example, ultrasonic transducers and more modern ones are integration of the sensors/actuators directly into the structure. The goal in the latter case may be to obtain vibration control. Often, the piezoelectric element is in the form of a thin plate, that is, the thickness of the piezoelectric material is much smaller than the wavelength of the elastic waves. This and the fact that the governing equations are fairly complicated (see the textbooks by Auld (1990) and Tiersten (1969) for the general three-dimensional theory) makes it attractive to approximate these layers in a simple fashion.

In the case of thin piezoelectric layers, various plate theories are often used. In the recent review article by Gopinathan et al. (2000), comparisons are made between the classical laminate theory and exact

* Corresponding author. Fax: +46-31-772-3827.
E-mail address: jonas.niklasson@me.chalmers.se (A.J. Niklasson).

0020-7683/03/$ - see front matter © 2003 Elsevier Science Ltd. All rights reserved.
doi:10.1016/S0020-7683(03)00151-3

three-dimensional solutions for a piezoelectric laminated beam. Several plate and shell theories for layered structures are also cited by Gopinathan et al. (2000). The finite element method (FEM) is developed for such problem by, for example, Tzou (1993) and Kim et al. (1996). Higher order piezoelectric plate theories and their applications are discussed in the recent review article by Wang and Yang (2000). Simplified equations of motion in thin piezoelectric coating layers are considered by, for example, Batra et al. (1996). Batra et al. (1996) consider a laminated plate with piezoelectric coatings which are approximated by a two-dimensional theory due to Tiersten (1993). A very similar problem using three-dimensional theory is considered by Gao et al. (1998).

In this paper, instead of using a plate theory, the thin piezoelectric layer is replaced by an approximate (or effective) boundary condition. The major benefit with this approach compared to using a plate theory is that no solution in the piezoelectric layer is needed at all. This could be particularly useful in FEM applications if the code do not include the option of piezoelectric materials. Approximate boundary and interface conditions have been considered by many authors in, for example, acoustics (Bövik, 1994), electromagnetics (Ammari and He, 1997; Idemen, 1988), and elastodynamics (Bövik, 1994; Niklasson et al., 2000a,b; Rokhlin and Huang, 1993). Bövik (1994) and Niklasson et al. (2000a,b), use series expansions of the fields through the thickness of the thin layer. By using the boundary and interface conditions together with the equations of motion of the thin layer, approximate boundary conditions are obtained by truncating the series. A similar technique based on series expansions of the fields is used by Ammari and He (1997). Rokhlin and Huang (1993) derive the transfer matrix of the layer and obtain approximate interface conditions by truncating a series expansion in the thickness h of the matrix. Even though the approach used by Rokhlin and Huang (1993) is somewhat different from the approach used by Niklasson et al. (2000b), the resulting interface conditions are identical. The technique used in the present paper is also based on series expansions of the fields through the thickness but is somewhat different from the approaches used by Bövik (1994) and Niklasson et al. (2000a,b).

The layout of the paper is as follows. In the next section, the basic equations governing wave propagation in piezoelectric materials are given. In Section 3, the derivation of the effective boundary conditions for a thin piezoelectric coating layer is presented. A technique previously used in the derivation of plate equations (Boström et al., 2001; Johansson, 1999) is employed. In Section 3.1, effective boundary conditions are derived for the one-dimensional case. Both the case when waves are excited normally to the interface by an electric voltage (actuator mode) and the case when the electric voltage is excited by an elastic wave of normal incidence (sensor mode) are considered. In Section 3.2, effective boundary conditions are derived for the two-dimensional case when the piezoelectric layer is acting as an actuator. The boundary conditions are truncated to different orders and used in some numerical examples presented in Section 4. In Section 4.1, one-dimensional cases with a coated isotropic half-space where the layer is acting as an actuator or sensor are presented. Here, the amplitude of the induced wave (actuator mode) and the amplitude of the induced voltage difference (sensor mode) are studied. In Section 4.2, the two-dimensional boundary conditions are used for a coated isotropic plate. Here, the propagation of guided in-plane (P-SV) waves in the layered plate is considered. In all numerical examples (both one-dimensional and two-dimensional), the solutions obtained from the approximate boundary conditions are compared with the exact solutions.

2. Basic equations

The motion of a piezoelectric material is governed by the three-dimensional stress equations of motion and the charge equation of electrostatics:

$$T_{ij,i} = \rho \ddot{u}_j, \quad D_{i,i} = 0, \tag{1}$$

where T_{ij}, u_j and D_i are the components of stress, mechanical displacement and electric displacement, respectively. ρ is the mass density, the summation convention is employed, and dot denotes differentiation with respect to time. The constitutive equations for a piezoelectric material are

$$T_{ij} = c_{ijkl}S_{kl} - e_{kij}E_k, \quad D_i = e_{ikl}S_{kl} + \epsilon_{ik}E_k, \tag{2}$$

where c_{ijkl}, e_{kij} and ϵ_{ik} are the components of elastic stiffness, piezoelectric coupling and dielectric permittivity, respectively. S_{kl} and E_k are the components of strain and electric field and may be expressed in terms of the elastic displacement u_i and the electric potential Φ by

$$S_{ij} = \frac{1}{2}(u_{i,j} + u_{j,i}), \quad E_i = -\Phi_{,i}, \tag{3}$$

where the quasi-static approximation has been used for the electric field. Combining Eqs. (1)–(3), the equations of motion and the charge equation of electrostatics may be written as

$$c_{ijkl}u_{k,li} + e_{kij}\Phi_{,ki} = \rho\ddot{u}_j, \quad e_{ikl}u_{k,li} - \epsilon_{ik}\Phi_{,ki} = 0. \tag{4}$$

The piezoelectric layer, in this paper, is made of a hexagonal crystal of the class $C_{6v} = 6mm$. If Voigt's abbreviated notation (Auld, 1990; Tiersten, 1969) is used, the material constants appearing in the constitutive equations (2) of this transversely isotropic material may be written as

$$[c_{IJ}] = \begin{pmatrix} c_{11} & c_{12} & c_{13} & 0 & 0 & 0 \\ c_{12} & c_{11} & c_{13} & 0 & 0 & 0 \\ c_{13} & c_{13} & c_{33} & 0 & 0 & 0 \\ 0 & 0 & 0 & c_{44} & 0 & 0 \\ 0 & 0 & 0 & 0 & c_{44} & 0 \\ 0 & 0 & 0 & 0 & 0 & c_{66} \end{pmatrix}, \quad c_{66} = \frac{1}{2}(c_{11} - c_{12}), \tag{5a}$$

$$[e_{iI}] = \begin{pmatrix} 0 & 0 & 0 & 0 & e_{15} & 0 \\ 0 & 0 & 0 & e_{15} & 0 & 0 \\ e_{31} & e_{31} & e_{33} & 0 & 0 & 0 \end{pmatrix}, \tag{5b}$$

$$[\epsilon_{ij}] = \begin{pmatrix} \epsilon_{11} & 0 & 0 \\ 0 & \epsilon_{11} & 0 \\ 0 & 0 & \epsilon_{33} \end{pmatrix}. \tag{5c}$$

3. Approximate boundary conditions

In this section three different cases are considered. The first is an one-dimensional case, where the piezoelectric layer is acting as an actuator and the second, which is also one-dimensional, is when the piezoelectric layer is acting as a sensor. Finally, a two-dimensional actuator case is considered. Approximate boundary conditions are derived for these three cases and will significantly reduce the complexity of the problems where they may replace the piezoelectric layers.

In the cases considered below, the piezoelectric layer (thickness h) is oriented such that the z-direction is normal to the layer and the xy-plane is chosen as the plane of isotropy of the transversely isotropic $6mm$ material (see Fig. 1). The piezoelectric strip is covered with silver electrodes on both sides. The silver electrodes are assumed to be of infinite conductivity and thin enough not to influence the mechanical behavior of the piezoelectric material. The piezoelectric material is assumed to be perfectly bonded to an elastic material as depicted in Fig. 1.

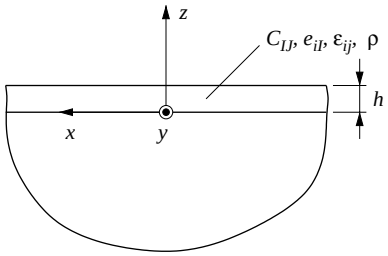

Fig. 1. A piezoelectric layer of thickness h perfectly bonded to an elastic material.

3.1. One-dimensional cases

Assume that all fields are independent of x and y and that the displacement components in the x- and y-directions are zero. The equation of motion and the charge equation for this one-dimensional case are then obtained from Eq. (4) as

$$c_{33}w_{,33} + e_{33}\Phi_{,33} = \rho\ddot{w}, \tag{6a}$$

$$e_{33}w_{,33} - \epsilon_{33}\Phi_{,33} = 0, \tag{6b}$$

where w is the displacement in the z-direction. The constitutive equations for the one-dimensional case are obtained from Eq. (2) as

$$T_{33} = c_{33}w_{,3} + e_{33}\Phi_{,3}, \tag{7a}$$

$$D_3 = e_{33}w_{,3} - \epsilon_{33}\Phi_{,3}. \tag{7b}$$

The displacement and the electric potential in the piezoelectric layer are expanded in the thickness coordinate as

$$w = \sum_{j=0}^{\infty} w_j z^j, \tag{8a}$$

$$\Phi = \sum_{j=0}^{\infty} \Phi_j z^j. \tag{8b}$$

Inserting the series expansions Eq. (8) into Eq. (6b) immediately gives

$$\Phi_j = \frac{e_{33}}{\epsilon_{33}} w_j, \quad j = 2, 3, \ldots \tag{9}$$

Further, elimination of the electric potential in Eq. (6) results in a partial differential equation in w:

$$\frac{\partial^2 w}{\partial z^2} - \frac{\rho}{\bar{c}} \frac{\partial^2 w}{\partial t^2} = 0, \tag{10}$$

where the piezoelectric effect gives rise to a stiffened elastic constant $\bar{c} = c_{33} + e_{33}^2/\epsilon_{33}$.

If the series expansion Eq. (8a) is inserted into Eq. (10) and every order of z is put equal to zero, the following relations are obtained:

$$w_{2j} = \frac{1}{(2j)!}\left(\frac{\rho}{\bar{c}}\right)^j \frac{\partial^{2j} w_0}{\partial t^{2j}}, \quad w_{2j+1} = \frac{1}{(2j+1)!}\left(\frac{\rho}{\bar{c}}\right)^j \frac{\partial^{2j} w_1}{\partial t^{2j}}, \quad j = 1, 2, \ldots \tag{11}$$

Now, only four unknowns remain in the series expansions (w_0, w_1, Φ_0, and Φ_1) and they will be determined by using the boundary conditions. It has to be decided if the piezoelectric layer should act as an actuator or a sensor. Both cases will be discussed starting with the case of an actuator.

3.1.1. Actuator case

The boundary conditions for the actuator case, with the interface between the two materials at $z = 0$ (see Fig. 1), are

$$z = h: \quad \Phi = V_1, \quad T_{33} = 0, \tag{12a}$$

$$z = 0: \quad \Phi = V_0, \quad T_{33} = T_{33}^{\mathrm{e}}, \quad w = w^{\mathrm{e}}, \tag{12b}$$

where w^{e} and T_{33}^{e} are the displacement and stress of the elastic material, respectively. V_0 and V_1 are voltages applied to the electrodes at $z = 0$ and $z = h$, respectively.

It is now easy to see that the boundary conditions at $z = 0$ immediately give

$$\Phi_0 = V_0, \quad w_0 = w^{\mathrm{e}} \tag{13}$$

and therefore only two unknowns remain to be determined. From the condition that $\Phi = V_1$ at $z = h$, the series expansion of Φ gives

$$\Phi_1 = \frac{V_1 - V_0}{h} - \left[\frac{e_{33}}{\epsilon_{33}} \sum_{j=1}^{\infty} \frac{h^{2j-1}}{(2j)!} \left(\frac{\rho}{\bar{c}}\right)^j \frac{\partial^{2j}}{\partial t^{2j}}\right] w^{\mathrm{e}} - \left[\frac{e_{33}}{\epsilon_{33}} \sum_{j=1}^{\infty} \frac{h^{2j}}{(2j+1)!} \left(\frac{\rho}{\bar{c}}\right)^j \frac{\partial^{2j}}{\partial t^{2j}}\right] w_1, \tag{14}$$

where Eqs. (9) and (11) have been used. By using the result for Φ_1 in the boundary condition $T_{33} = 0$ at $z = h$, the following is obtained for w_1:

$$\begin{aligned} &\left[c_{33} + \sum_{j=1}^{\infty} \left(\bar{c} - \frac{e_{33}^2}{(2j+1)\epsilon_{33}}\right) \frac{h^{2j}}{(2j)!} \left(\frac{\rho}{\bar{c}}\right)^j \frac{\partial^{2j}}{\partial t^{2j}}\right] w_1 \\ &\quad = -\frac{e_{33}(V_1 - V_0)}{h} - \left[\sum_{j=1}^{\infty} \left(\bar{c} - \frac{e_{33}^2}{(2j)\epsilon_{33}}\right) \frac{h^{2j-1}}{(2j-1)!} \left(\frac{\rho}{\bar{c}}\right)^j \frac{\partial^{2j}}{\partial t^{2j}}\right] w^{\mathrm{e}}. \end{aligned} \tag{15}$$

At $z = 0$ the elastic stress T_{33}^{e} reduces to $T_{33}^{\mathrm{e}} = c_{33} w_1 + e_{33} \Phi_1$. If Φ_1 is inserted into this expression, T_{33}^{e} may be written as

$$T_{33}^{\mathrm{e}} = \frac{e_{33}(V_1 - V_0)}{h} + \left[c_{33} - \frac{e_{33}^2}{\epsilon_{33}} \sum_{j=1}^{\infty} \frac{h^{2j}}{(2j+1)!} \left(\frac{\rho}{\bar{c}}\right)^j \frac{\partial^{2j}}{\partial t^{2j}}\right] w_1 - \left[\frac{e_{33}^2}{\epsilon_{33}} \sum_{j=1}^{\infty} \frac{h^{2j-1}}{(2j)!} \left(\frac{\rho}{\bar{c}}\right)^j \frac{\partial^{2j}}{\partial t^{2j}}\right] w^{\mathrm{e}}, \tag{16}$$

where w_1 is given by Eq. (15). It should be noted that so far no truncations have been made to the series expansions. The approximate boundary conditions are now obtained as truncations for different orders of h.

The three lowest order approximate boundary conditions obtained from Eqs. (15) and (16) by truncation of the series expansion are

First:

$$T_{33}^{\mathrm{e}} = \rho h \frac{\partial^2}{\partial t^2} \left[\frac{e_{33}}{2c_{33}} (V_1 - V_0) - w^{\mathrm{e}}\right], \quad z = 0. \tag{17}$$

Second:

$$\left[6c_{33}+\rho h^2\left(2+\frac{c_{33}}{\bar{c}}\right)\frac{\partial^2}{\partial t^2}\right]T_{33}^{\mathrm{e}}=3\rho h\frac{\partial^2}{\partial t^2}[e_{33}(V_1-V_0)-2c_{33}w^{\mathrm{e}}],\quad z=0. \tag{18}$$

Third:

$$\left[24c_{33}+4\rho h^2\left(2+\frac{c_{33}}{\bar{c}}\right)\frac{\partial^2}{\partial t^2}\right]T_{33}^{\mathrm{e}} = \rho h\frac{\partial^2}{\partial t^2}\left[e_{33}\left[12+\frac{\rho h^2}{\bar{c}}\frac{\partial^2}{\partial t^2}\right](V_1-V_0)-\left[24c_{33}+2\rho h^2\left(1+\frac{c_{33}}{\bar{c}}\right)\frac{\partial^2}{\partial t^2}\right]w^{\mathrm{e}}\right],\quad z=0. \tag{19}$$

These three different order of truncation will be used in numerical calculations in a subsequent section to show the limitations of the approximate boundary conditions. It should be noted that it is straightforward to derive higher order approximate boundary conditions even though this is not done here.

3.1.2. Sensor case

The same configuration as in the actuator case above is used but the boundary conditions for this case are

$$z=h:\quad D_3=0,\quad T_{33}=0, \tag{20a}$$

$$z=0:\quad D_3=0,\quad T_{33}=T_{33}^{\mathrm{e}},\quad w=w^{\mathrm{e}}. \tag{20b}$$

The only difference from the actuator case is that the electrical boundary conditions are changed to restrictions on the electric displacement instead of the electric potential. The reason why $D_3=0$ at the boundaries is that the piezoelectric layer is assumed to be bonded with silver electrodes with infinite conductivity.

The boundary conditions on the surface $z=0$ immediately give for the displacement that

$$w_0=w^{\mathrm{e}} \tag{21}$$

and thus leaves only three unknowns to be determined. Note that even though there are four boundary conditions left, this will not be a problem since the two conditions on the electrical displacement yields the same relationship between Φ_1 and w_1. From $D_3=0$ at $z=0$ it follows that

$$\Phi_1=\frac{e_{33}}{\epsilon_{33}}w_1 \tag{22}$$

and it is also easy to see, if (9) is used, that the boundary condition $D_3=0$ at $z=h$ gives the same relation. Inserted into the expression for T_{33}, Eq. (7a), at $z=0$, the resulting stress boundary condition is

$$T_{33}=\bar{c}w_1=T_{33}^{\mathrm{e}},\quad z=0. \tag{23}$$

This means that the only unknown left to be determined is w_1. This can be done by using the stress boundary condition at $z=h$, and the result is

$$\left[\sum_{j=0}^{\infty}\frac{h^{2j}}{(2j)!}\left(\frac{\rho}{\bar{c}}\right)^j\frac{\partial^{2j}}{\partial t^{2j}}\right]w_1=-\left[\sum_{j=1}^{\infty}\frac{h^{2j-1}}{(2j-1)!}\left(\frac{\rho}{\bar{c}}\right)^j\frac{\partial^{2j}}{\partial t^{2j}}\right]w_0. \tag{24}$$

If this is inserted into the stress boundary condition at $z=0$, Eq. (23), the following relation for the elastic stress T_{33}^{e} is obtained:

$$\left[\sum_{j=0}^{\infty}\frac{h^{2j}}{(2j)!}\left(\frac{\rho}{\bar{c}}\right)^{j}\frac{\partial^{2j}}{\partial t^{2j}}\right]T_{33}^{e}=-\bar{c}\left[\sum_{j=1}^{\infty}\frac{h^{2j-1}}{(2j-1)!}\left(\frac{\rho}{\bar{c}}\right)^{j}\frac{\partial^{2j}}{\partial t^{2j}}\right]w^{e}, \tag{25}$$

where the relation $w_0 = w^e$ also has been used. It should be noted, as in the actuator case, that so far no truncations have been made to the series expansions. But now, when the final expression for the elastic stress at the interface between the piezoelectric layer and the elastic material has been obtained, it may be truncated to obtain approximate boundary conditions at different orders.

To the lowest order of truncation of Eq. (25), the approximate boundary condition for the sensor case is

$$T_{33}^{e}=-\rho h\frac{\partial^{2}w^{e}}{\partial t^{2}},\quad z=0. \tag{26}$$

It is noted that to the lowest order, only the inertia of the piezoelectric layer is taken into account. The second lowest order of truncation of Eq. (25) yields the approximate boundary condition

$$\left[2+\frac{\rho h^{2}}{\bar{c}}\frac{\partial^{2}}{\partial t^{2}}\right]T_{33}^{e}=-2\rho h\frac{\partial^{2}w^{e}}{\partial t^{2}},\quad z=0, \tag{27}$$

where now the elastic and electric properties of the layer appear in $\bar{c}$. The third lowest order of truncation of Eq. (25) yields the following approximate boundary condition:

$$\left[6+\frac{3h^{2}\rho}{\bar{c}}\frac{\partial^{2}}{\partial t^{2}}\right]T_{33}^{e}=-\rho h\frac{\partial^{2}}{\partial t^{2}}\left[6+\frac{h^{2}\rho}{\bar{c}}\frac{\partial^{2}}{\partial t^{2}}\right]w^{e},\quad z=0. \tag{28}$$

The desired output in the sensor case is the difference in voltage between the layer's two surfaces. By using Eqs. (8), (9), (11), and (24), the following expression is obtained

$$\left[\sum_{j=0}^{\infty}\frac{h^{2j}}{(2j)!}\left(\frac{\rho}{\bar{c}}\right)^{j}\frac{\partial^{2j}}{\partial t^{2j}}\right](V_1-V_0)=-\frac{e_{33}}{\epsilon_{33}}\left[\sum_{j=1}^{\infty}\frac{h^{2j}}{(2j)!}\left(\frac{\rho}{\bar{c}}\right)^{j}\frac{\partial^{2j}}{\partial t^{2j}}\right]w^{e}. \tag{29}$$

The three lowest order truncations of Eq. (29) are

First:

$$V_1-V_0=-\frac{e_{33}}{\epsilon_{33}}\frac{h^{2}}{2!}\frac{\rho}{\bar{c}}\frac{\partial^{2}w^{e}}{\partial t^{2}},\quad z=0, \tag{30}$$

Second:

$$\left[1+\frac{h^{2}}{2!}\frac{\rho}{\bar{c}}\frac{\partial^{2}}{\partial t^{2}}\right](V_1-V_0)=-\frac{e_{33}}{\epsilon_{33}}\frac{h^{2}}{2!}\frac{\rho}{\bar{c}}\frac{\partial^{2}w^{e}}{\partial t^{2}},\quad z=0, \tag{31}$$

Third:

$$\left[1+\frac{h^{2}}{2!}\frac{\rho}{\bar{c}}\frac{\partial^{2}}{\partial t^{2}}\right](V_1-V_0)=-\frac{e_{33}}{\epsilon_{33}}\left[\frac{h^{2}}{2!}\frac{\rho}{\bar{c}}\frac{\partial^{2}}{\partial t^{2}}+\frac{h^{4}}{4!}\frac{\rho^{2}}{\bar{c}^{2}}\frac{\partial^{4}}{\partial t^{4}}\right]w^{e},\quad z=0. \tag{32}$$

3.2. Two-dimensional actuator case

In this section the same analysis as in the one-dimensional case is performed for the two-dimensional case. This means that the x-direction is also included in the calculations. Since the piezoelectric layer is isotropic in the xy-plane it does not matter whether the x- or the y-coordinate is included. Also, only the

actuator case will be treated in this section. Since the expressions obtained in the two-dimensional case are much more complicated than in the one-dimensional case, most details are omitted in this section.

If it is assumed that all fields are independent of y and the displacement in the y-direction is zero, the equations governing the motion of the piezoelectric layer are

$$c_{11}\frac{\partial^2 u}{\partial x^2}+(c_{13}+c_{44})\frac{\partial^2 w}{\partial x\,\partial z}+c_{44}\frac{\partial^2 u}{\partial z^2}+(e_{15}+e_{31})\frac{\partial^2 \Phi}{\partial x\,\partial z}=\rho\frac{\partial^2 u}{\partial t^2}, \tag{33a}$$

$$c_{44}\frac{\partial^2 w}{\partial x^2}+(c_{13}+c_{44})\frac{\partial^2 u}{\partial x\,\partial z}+c_{33}\frac{\partial^2 w}{\partial z^2}+e_{15}\frac{\partial^2 \Phi}{\partial x^2}+e_{33}\frac{\partial^2 \Phi}{\partial z^2}=\rho\frac{\partial^2 w}{\partial t^2}, \tag{33b}$$

$$e_{15}\frac{\partial^2 w}{\partial x^2}+(e_{15}+e_{31})\frac{\partial^2 u}{\partial x\,\partial z}+e_{33}\frac{\partial^2 w}{\partial z^2}-\epsilon_{11}\frac{\partial^2 \Phi}{\partial x^2}-\epsilon_{33}\frac{\partial^2 \Phi}{\partial z^2}=0. \tag{33c}$$

Here, u is the displacement in the x-direction and w is the displacement in the z-direction. The relevant constitutive equations in this case are

$$T_{31}=c_{44}\left(\frac{\partial w}{\partial x}+\frac{\partial u}{\partial z}\right)+e_{15}\frac{\partial \Phi}{\partial x}, \tag{34a}$$

$$T_{33}=c_{13}\frac{\partial u}{\partial x}+c_{33}\frac{\partial w}{\partial z}+e_{33}\frac{\partial \Phi}{\partial z}. \tag{34b}$$

The constitutive equations for the electrical displacements are not listed here as they are of no immediate interest in the case of the actuator.

Next, series expansions of the displacements and the electrical potential in the piezoelectric layer are introduced as

$$u=\sum_{j=0}^{\infty}u_j z^j,\quad w=\sum_{j=0}^{\infty}w_j z^j,\quad \Phi=\sum_{j=0}^{\infty}\Phi_j z^j. \tag{35}$$

Exactly as in the one-dimensional case, the series expansions are now inserted into the equations of motion Eq. (33). By using these equations it is possible to eliminate all unknowns but the six of lowest order in the series expansions (u_0, w_0, Φ_0, u_1, w_1, and Φ_1). The remaining six unknowns will be determined by using the boundary conditions for this problem. The boundary conditions are

$$z=h:\quad \Phi=V_1,\quad T_{31}=0,\quad T_{33}=0, \tag{36a}$$

$$z=0:\quad \Phi=V_0,\quad T_{31}=T_{31}^{\mathrm{e}},\quad T_{33}=T_{33}^{\mathrm{e}},\quad u=u^{\mathrm{e}},\quad w=w^{\mathrm{e}}, \tag{36b}$$

where u^{e} and w^{e} are the displacements in the x- and z-directions, respectively, of the elastic material. V_0 and V_1 are known electrical potentials and if the silver electrodes on the piezoelectric material are shorted, they are equal and may be set to zero. This is done in the numerical examples in Section 4.2.

The six remaining unknown expansion functions (u_0, w_0, Φ_0, u_1, w_1, and Φ_1) are determined from the boundary conditions $\Phi=V_1$, $T_{31}=0$, and $T_{33}=0$ at $z=h$ and $\Phi=V_0$, $u=u^{\mathrm{e}}$, and $w=w^{\mathrm{e}}$ at $z=0$. When this has been done, only two boundary conditions at $z=0$ remain:

$$z=0:\quad T_{31}=T_{31}^{\mathrm{e}},\quad T_{33}=T_{33}^{\mathrm{e}}. \tag{37}$$

At $z=0$, T_{31} and T_{33} from Eq. (34), with the series expansions inserted, may be written as

$$T_{31}=c_{44}\left(u_1+\frac{\partial w_0}{\partial x}\right)+e_{15}\frac{\partial \Phi_0}{\partial x}, \tag{38a}$$

$$T_{33} = c_{13}\frac{\partial u_0}{\partial x} + c_{33}w_1 + e_{33}\Phi_1. \tag{38b}$$

By insertion of the already known expansion functions u_0, w_0, Φ_0, u_1, w_1, and Φ_1, into Eq. (38) and truncation to different orders, approximate boundary conditions are finally obtained from Eq. (37).

The lowest order approximate boundary conditions may be written as

$$T_{31}^{\mathrm{e}} = \left(e_{31} - e_{33}\frac{c_{13}}{c_{33}}\right)\frac{\partial}{\partial x}(V_1 - V_0) - h\left[\rho\frac{\partial^2}{\partial t^2} - \left(c_{11} - \frac{c_{13}^2}{c_{33}}\right)\frac{\partial^2}{\partial x^2}\right]u^{\mathrm{e}}, \quad z = 0, \tag{39a}$$

$$T_{33}^{\mathrm{e}} = \frac{h}{2c_{33}}\left[(c_{33}e_{31} - c_{13}e_{33})\frac{\partial^2}{\partial x^2} + e_{33}\rho\frac{\partial^2}{\partial t^2}\right](V_1 - V_0) - h\rho\frac{\partial^2 w^{\mathrm{e}}}{\partial t^2}, \quad z = 0. \tag{39b}$$

The lowest order approximate boundary conditions, Eq. (39), are obtained by neglecting all terms of order higher than h. It is easy to see that if the x-dependence is omitted, the same equation as in the one-dimensional case is obtained from Eq. (39b), cf. Eq. (17). The second lowest order approximate boundary conditions are obtained by neglecting all terms of order higher than h^2, and finally in the third order all terms of order higher than h^3 are neglected. The second and third order approximate boundary conditions are not shown explicitly here for brevity, but they are discussed together with some numerical examples in Section 4. These higher order approximate boundary conditions are derived with the aid of the program *Mathematica* (Wolfram, 1999) since the expressions get rather complicated.

4. Numerical examples

In this section, numerical examples are given for one-dimensional sensor and actuator cases and for two-dimensional guided waves in a layered plate. The approximate boundary conditions derived in Section 3 are used to obtain approximate solutions. Different order of truncation of the effective boundary conditions are compared to each other as well as to the corresponding exact solutions. The main goal here is to investigate the validity of the approximations.

In all the examples below, the piezoelectric material is taken as PZT-2 (lead zirconate titanate) and the isotropic material is steel. The material properties of PZT-2 (class 6*mm* with the *xy*-plane as the plane of isotropy) are given in Table 1 (Auld, 1990). The Lamé constants of the isotropic steel are $\lambda = 121$ GPa, $\mu = 80.8$ GPa (or Young's modulus $E = 210$ GPa and Poisson's ratio $v = 0.3$) and the density is $\rho^{\mathrm{e}} = 7870$ kg/m^3.

4.1. One-dimensional cases

In this section some numerical results for the one-dimensional sensor and actuator cases are presented. Below, all fields are assumed to be time harmonic with the time dependence $\exp(-\mathrm{i}\omega t)$. The factor $\exp(-\mathrm{i}\omega t)$ is, however, suppressed throughout. Different order of approximate boundary conditions are used in a simple actuator and sensor example to show their limitations.

Table 1
Material properties of PZT-2 (c_{IJ} in GPa, e_{iJ} in C/m^2, $\epsilon_0 = 8.854 \times 10^{-12}$ C/V m, and ρ in kg/m^3)

c_{11}	c_{12}	c_{13}	c_{33}	c_{44}	e_{15}	e_{31}	e_{33}	ϵ_{11}/ϵ_0	ϵ_{33}/ϵ_0	ρ
135	67.0	68.1	113	22.2	9.8	−1.9	9.0	540	260	7600

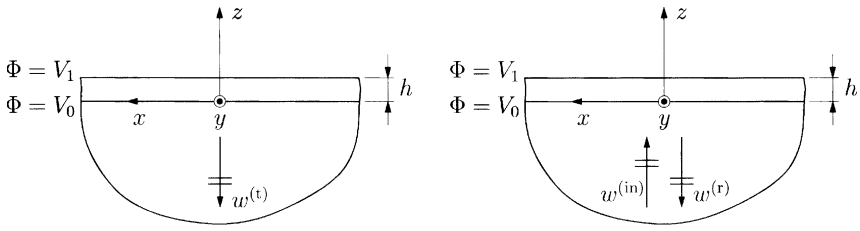

Fig. 2. A piezoelectric layer of thickness h acting as an actuator or a sensor.

4.1.1. Actuator case

Fig. 2(a) shows an isotropic half-space coated by a piezoelectric layer of thickness h. A plane elastic wave is induced in the half-space by applying a voltage $\Phi = V_1$ to the upper (free) surface $z = h$ of the layer and a voltage $\Phi = V_0$ to the lower surface $z = 0$ of the layer. In this section, the amplitude of the transmitted wave ($w^{(t)}$ in the figure) obtained from the exact solution is compared to the amplitude obtained when the layer is replaced by approximate boundary conditions of different orders.

The difference between the voltages at the layer's surfaces, $V_1 - V_0$, is assumed to be

$$V_1 - V_0 = \Delta V. \tag{40}$$

The equations governing one-dimensional (time harmonic) motion in the isotropic half-space are

$$\frac{\partial T_{33}^{e}}{\partial z} + \rho^{e}\omega^2 w^{e} = 0, \quad T_{33}^{e} = (\lambda + 2\mu)\frac{\partial w^{e}}{\partial z}. \tag{41}$$

From Eq. (41) and radiation conditions at infinity, the total displacement field in the isotropic half-space is

$$w^{e} = A_2 e^{-ik_z^{e} z}, \tag{42}$$

where the wavenumber in the elastic half-space k_z^{e} is given by

$$k_z^{e} = \omega\sqrt{\frac{\rho^{e}}{\lambda + 2\mu}}. \tag{43}$$

Note that the displacement field in the isotropic half-space consists of the transmitted field only, i.e., a plane wave propagating in the negative z-direction.

In order to obtain the exact solution, i.e., the exact expression for A_2, the displacement field and potential in the piezoelectric layer are obtained from Eqs. (6b) and (10), assuming time harmonic conditions, as

$$w = A_1 e^{ik_z z} + B_1 e^{-ik_z z}, \tag{44}$$

$$\Phi = \frac{e_{33}}{\epsilon_{33}} w + C_1 z + C_2, \tag{45}$$

where k_z is the wavenumber in the piezoelectric layer, i.e.,

$$k_z = \omega\sqrt{\frac{\rho}{\bar{c}}}. \tag{46}$$

The constants A_1, B_1, A_2, C_1, and C_2 are determined by the actuator case boundary conditions Eq. (12). The expression for the exact amplitude of the transmitted wave, A_2, is given by

$$A_2 = \left[2\mathrm{i}\left(\frac{e_{33}}{\epsilon_{33}} \sin(k_z h) - \frac{\bar{c} k_z h}{e_{33}} \cos(k_z h) \right) \frac{(\bar{c} k_z (1 - \mathrm{e}^{-\mathrm{i}k_z h}) - (\lambda + 2\mu) k_z^{\mathrm{e}})}{2\bar{c} k_z (1 - \cos(k_z h))} + \frac{e_{33}}{\epsilon_{33}} (\mathrm{e}^{-\mathrm{i}k_z h} - 1) + \frac{\mathrm{i}\bar{c} k_z h}{e_{33}} \mathrm{e}^{-\mathrm{i}k_z h} \right]^{-1} \Delta V. \tag{47}$$

Insertion of Eqs. (40) and (42) into the approximate boundary condition of lowest order (17) results in the approximation

$$A_2 = \frac{e_{33} \bar{c} h k_z^2}{2c_{33}(\bar{c} h k_z^2 + \mathrm{i} k_z^{\mathrm{e}} (\lambda + 2\mu))} \Delta V. \tag{48}$$

If the second lowest order boundary condition Eq. (18) is used, the result is

$$A_2 = \frac{3 e_{33} \bar{c} h k_z^2}{6c_{33} \bar{c} h k_z^2 + \mathrm{i} k_z^{\mathrm{e}} (\lambda + 2\mu)(6c_{33} - h^2 k_z^2 (2\bar{c} + c_{33}))} \Delta V, \tag{49}$$

Finally, if Eqs. (40) and (42) are inserted into the approximate boundary condition of the third order Eq. (19), the resulting amplitude A_2 is

$$A_2 = \frac{e_{33} \bar{c} h k_z^2 (12 - h^2 k_z^2)}{2\bar{c} h k_z^2 (12 c_{33} - h^2 k_z^2 (\bar{c} + c_{33})) + 4\mathrm{i} k_z^{\mathrm{e}} (\lambda + 2\mu)(6c_{33} - h^2 k_z^2 (2\bar{c} + c_{33}))} \Delta V. \tag{50}$$

If Eq. (47) is rewritten and the numerator and denominator are series expanded, truncations yield the approximate expressions Eqs. (48)–(50).

The amplitude of the wave generated in the half-space, A_2, for the actuator case is shown in Fig. 3. $a_2 = \sqrt{c_{33}/\epsilon_{33}}\, A_2/\Delta V$ is plotted as a function of $k_z h$ in polar form, i.e., $a_2 = |a_2| \exp(\mathrm{i} \arg(a_2))$ with $|a_2|$ in Fig. 3(a) and $\arg(a_2)$ in Fig. 3(b). The exact solution is shown together with the three lowest order of approximations derived above. As is seen in the figure, the amplitude obtained from the first (lowest) approximate boundary condition, Eq. (48), is only in good agreement with the exact amplitude when $k_z h < 0.3$. It is also seen that the phase is in better agreement than the absolute value. The second and third approximate boundary conditions, Eqs. (49) and (50), offer significant improvements. The absolute value of the amplitudes are in very good agreement with the exact one when $k_z h < 1$. The phase of the second order approximation, Eq. (49), starts to break down much earlier than the phase of the third order approximation, Eq. (50), (see Fig. 3(b)). From the figure, it is seen that the second order approximation starts to break down when $k_z h \approx 0.5$ and the third order approximation when $k_z h \approx 1$.

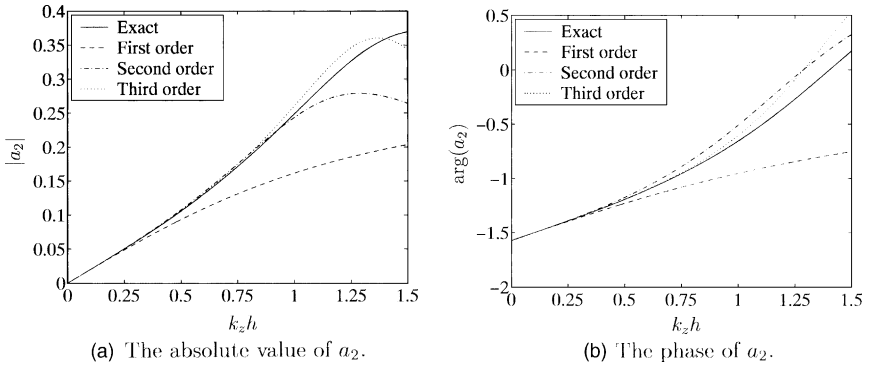

(a) The absolute value of a_2. (b) The phase of a_2.

Fig. 3. The absolute value and phase of $a_2 = \sqrt{c_{33}/\epsilon_{33}}\, A_2/\Delta V$.

4.1.2. Sensor case

Here, the same configuration as in the previous subsection is considered but instead of inducing a wave in the isotropic half-space by applying voltages to the layer's surfaces, a plane wave incident in the half-space ($w^{(\mathrm{in})}$) is inducing a difference in the voltages V_0 and V_1 (see Fig. 2(b)). Comparisons between $\Delta V = V_1 - V_0$ obtained from the exact solution and approximate boundary conditions of various orders are made.

The displacement field in the elastic half-space may be written as the sum of the incident wave and the reflected wave as (see Eq. (41))

$$w^{\mathrm{e}} = A_0 \mathrm{e}^{\mathrm{i}k_z^{\mathrm{e}} z} + A_2 \mathrm{e}^{-\mathrm{i}k_z^{\mathrm{e}} z}. \tag{51}$$

The difference in the voltages $\Delta V = V_1 - V_0$ will now be determined using the exact equations as well as different orders of approximate boundary conditions.

As in the previous section, the displacement field and the electric potential in the piezoelectric layer are obtained from Eqs. (6b) and (10) as

$$w = A_1 \mathrm{e}^{\mathrm{i}k_z z} + B_1 \mathrm{e}^{-\mathrm{i}k_z z}, \tag{52}$$

$$\Phi = \frac{e_{33}}{\epsilon_{33}} w + C_1 z + C_2. \tag{53}$$

The constants A_1, B_1, A_2, C_1, and C_2 are determined by the sensor case boundary conditions Eq. (20). The exact expression for ΔV is then given by

$$\Delta V = \frac{2e_{33}(\lambda + 2\mu)k_z^{\mathrm{e}}(1 - \cos(k_z h))}{\epsilon_{33}((\lambda + 2\mu)k_z^{\mathrm{e}} \cos(k_z h) - \mathrm{i}\bar{c}k_z \sin(k_z h))} A_0. \tag{54}$$

If Eq. (51) is inserted into the lowest order boundary condition, Eq. (26), and Eq. (30) is used, the difference in the voltages, ΔV, is given by

$$\Delta V = \frac{e_{33}(\lambda + 2\mu)k_z^{\mathrm{e}} k_z^2 h^2}{\epsilon_{33}((\lambda + 2\mu)k_z^{\mathrm{e}} - \mathrm{i}\bar{c}k_z^2 h)} A_0. \tag{55}$$

The second lowest order boundary condition, Eq. (27), combined with the corresponding expression for ΔV, Eq. (31), yield

$$\Delta V = \frac{2e_{33}(\lambda + 2\mu)k_z^{\mathrm{e}} k_z^2 h^2}{\epsilon_{33}((\lambda + 2\mu)k_z^{\mathrm{e}}(2 - k_z^2 h^2) - 2\mathrm{i}\bar{c}k_z^2 h)} A_0. \tag{56}$$

Finally, insertion of Eq. (51) into the third order boundary condition, Eq. (28), combined with Eq. (32) result in the expression

$$\Delta V = \frac{e_{33}(\lambda + 2\mu)k_z^{\mathrm{e}} k_z^2 h^2 (12 - k_z^2 h^2)}{2\epsilon_{33}(3(\lambda + 2\mu)k_z^{\mathrm{e}}(2 - k_z^2 h^2) - \mathrm{i}\bar{c}k_z^2 h(6 - k_z^2 h^2))} A_0. \tag{57}$$

It is easy to see that series expansions of the numerator and denominator in Eq. (54) and truncation to different orders result in the approximate expressions Eqs. (55)–(57).

In Fig. 4, the absolute value and phase of $\Delta v = \sqrt{\epsilon_{33}/c_{33}}\, \Delta V/A_0$ are shown as a functions of $k_z h$. The same conclusions may be drawn from Figs. 3 and 4, the first approximation is valid up to $k_z h \approx 0.3$, the second order up to $k_z h \approx 0.5$, and the third order up to $k_z h \approx 1$.

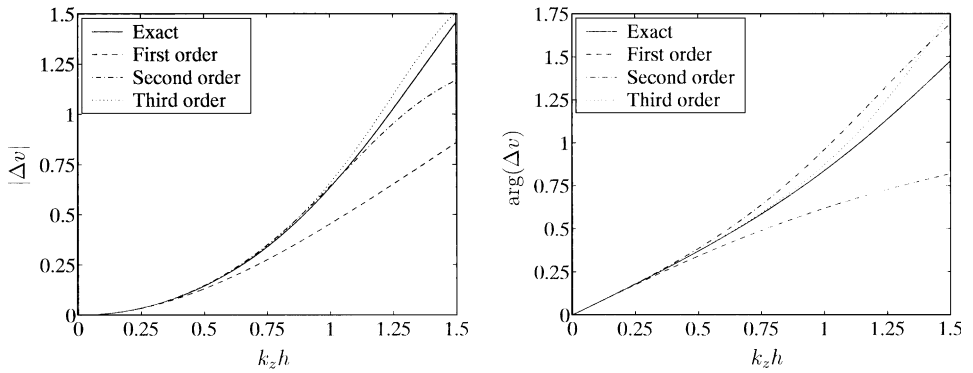

(a) The absolute value of Δv. (b) The phase of Δv.

Fig. 4. The absolute value and phase of $\Delta v = \sqrt{\epsilon_{33}/c_{33}}\,\Delta V/A_0$.

4.2. Two-dimensional case

In this section the two-dimensional approximate boundary conditions are evaluated. The calculations are made for the case when two plates, one piezoelectric and one elastic, are perfectly bonded to each other. Dispersion relations are calculated for different order of truncations when the electrodes are shorted, i.e., $V_0 = V_1 = 0$ (see Fig. 5). They are then compared to the exact solution, which is obtained from the two-dimensional equations of piezoelectricity and elasticity. The thickness ratio of the piezoelectric layer and the elastic plate is varied in order to show the limitations of the approximate boundary conditions.

The dispersion relation for the exact case is obtained by using the two-dimensional equations of motion, Eq. (33), combined with the two-dimensional elastic equations of motion and the boundary/interface conditions appropriate for this case. The equations of motion and constitutive relations for in-plane motion of an isotropic, homogeneous elastic material are

$$\frac{\partial T_{11}^{\mathrm{e}}}{\partial x} + \frac{\partial T_{31}^{\mathrm{e}}}{\partial z} = \rho^{\mathrm{e}} \frac{\partial^2 u^{\mathrm{e}}}{\partial t^2}, \quad \frac{\partial T_{31}^{\mathrm{e}}}{\partial x} + \frac{\partial T_{33}^{\mathrm{e}}}{\partial z} = \rho^{\mathrm{e}} \frac{\partial^2 w^{\mathrm{e}}}{\partial t^2}, \tag{58a}$$

$$T_{11}^{\mathrm{e}} = (\lambda + 2\mu)\frac{\partial u^{\mathrm{e}}}{\partial x} + \lambda \frac{\partial w^{\mathrm{e}}}{\partial z}, \quad T_{31}^{\mathrm{e}} = \mu\left(\frac{\partial u^{\mathrm{e}}}{\partial z} + \frac{\partial w^{\mathrm{e}}}{\partial x}\right), \quad T_{33}^{\mathrm{e}} = \lambda \frac{\partial u^{\mathrm{e}}}{\partial x} + (\lambda + 2\mu)\frac{\partial w^{\mathrm{e}}}{\partial z}. \tag{58b}$$

u^{e} is the displacement in the x-direction and w^{e} is the displacement in the z-direction in the elastic material. λ and μ are the Lamé constants. The boundary conditions governing this case are

$$z = h: \quad T_{31} = 0, \quad T_{33} = 0, \quad \Phi = 0, \tag{59a}$$

$$z = 0: \quad T_{31} = T_{31}^{\mathrm{e}}, \quad T_{33} = T_{33}^{\mathrm{e}}, \quad \Phi = 0, \quad u = u^{\mathrm{e}}, \quad w = w^{\mathrm{e}}, \tag{59b}$$

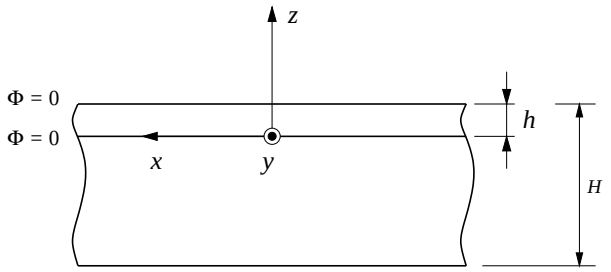

Fig. 5. A piezoelectric layer with shorted electrodes perfectly bonded to an elastic plate.

$$z = -(H-h): \quad T_{31}^{e} = 0, \quad T_{33}^{e} = 0. \tag{59c}$$

Briefly, the exact dispersion relation is obtained as follows. First, general solutions are obtained in the piezoelectric and elastic layers from Eqs. (33) and (58), respectively, assuming that all fields are in the form $F(z)\exp(\mathrm{i}(k_x x - \omega t))$. Then, the boundary and interface conditions Eq. (59) yield a homogeneous system of equations for the unknown integration constants of the layers. The requirement that a non-trivial solution should exist, i.e., that the determinant of the system matrix is zero, yields the exact dispersion relation.

When using the approximate boundary conditions, the piezoelectric layer is reduced to two approximate boundary conditions that are applied to the elastic material. By doing this, the problem is reduced to solving the equations of motion in the elastic plate, Eq. (58a), together with the boundary conditions

$$z = 0: \quad T_{31}^{e} = T_{31}^{\mathrm{eff}}, \quad T_{33}^{e} = T_{33}^{\mathrm{eff}}, \tag{60a}$$

$$z = -(H-h): \quad T_{31}^{e} = 0, \quad T_{33}^{e} = 0. \tag{60b}$$

Above, T_{31}^{eff} and T_{33}^{eff} are the approximate boundary conditions replacing the piezoelectric layer with $V_0 = V_1 = 0$ in this case. The lowest order approximate boundary conditions for the two-dimensional case are given by Eq. (39). To obtain the dispersion relation, the procedure is the same as in the exact case. First, a general solution is obtained in the elastic plate assuming that all fields are in the form $F(z)\exp(\mathrm{i}(k_x x - \omega t))$. When the general solution is inserted into the boundary conditions (60), the result is a homogeneous system of equations for the integration constants. The requirement that a non-trivial solution should exist, yields the dispersion relation.

In Fig. 6, the dispersion curves when $h = 0.1H$ are shown. Here it can be seen that even the first order approximation is in excellent agreement with the exact solution for the first mode. For the second mode, the first approximation is very good up to $k_x H = 3$ ($k_x h = 0.3$) but the second and third order approximation is very good in the whole interval. All approximate solutions capture the cut-off frequency of the third mode well, but the first and second order approximations are clearly not as good as the third order approximation at higher frequencies.

In Fig. 7, $h = 0.2H$, which makes the influence from the piezoelectric material greater and therefore the results in this case are not expected to be as good as they are in Fig. 6. For the first mode it can be seen that the first order approximation is very good up to at least $k_x H = 3$ ($k_x h = 0.6$). The third order approximation is very good in the whole interval. For the second mode the first approximation is good up to $k_x H = 1.75$ ($k_x h = 0.35$), while the second approximation matches the exact curve well up to $k_x H = 2.25$ ($k_x h = 0.45$).

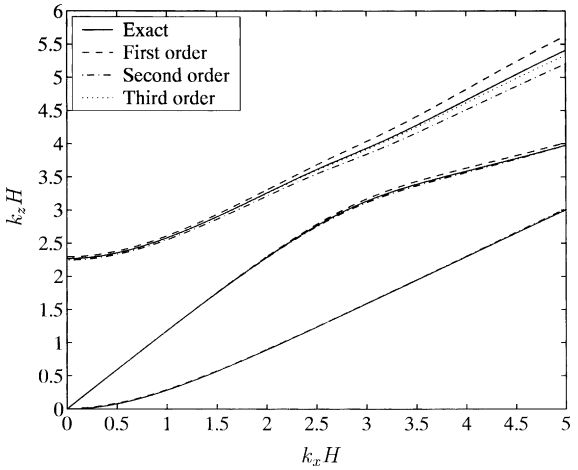

Fig. 6. Dispersion curves when $h = 0.1H$.

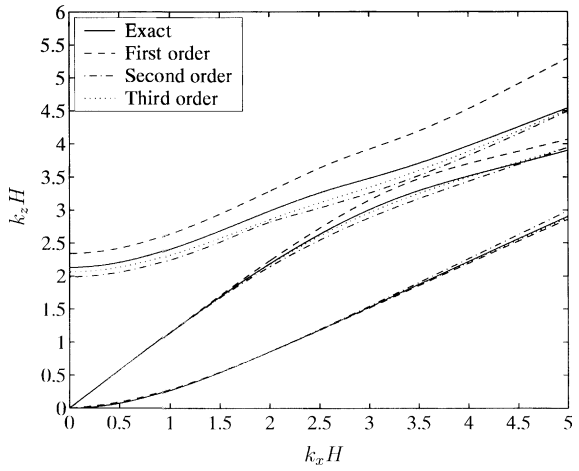

Fig. 7. Dispersion curves when $h = 0.2H$.

The third order approximation is very good in the whole interval. For the third mode it is seen that the first approximation results in a fairly large error in the cut-off frequency and this is the case for the second and third approximations as well, even if the errors are much smaller than the error in the first approximation. The main reason for these relatively large errors in the third mode is that a significant portion of the plate is modeled by the approximate boundary conditions, which are similar to using a plate theory. In order to model the third mode more accurately, higher order approximate boundary conditions than the ones considered in this paper should be used. See Boström et al. (2001) and Johansson (1999) for more thorough discussions on higher order plate theory using derivation techniques similar to the one used in this paper.

Finally note that the main reason why the approximations appear to be much better when $h = 0.1H$ than when $h = 0.2H$ for all modes is the scaling of the axes in Figs. 6 and 7. If the dispersion curves are viewed as $k_x h$ versus $k_z h$ instead of $k_x H$ versus $k_z H$, the approximations are about as good in both cases ($h = 0.1H$ and $h = 0.2H$).

5. Conclusions

This paper has been discussing the derivation of approximate boundary conditions for a thin piezoelectric layer. The derivation is performed by expanding the displacement and electric potential in power series in the thickness coordinate. The displacement and potential are then inserted into the equations of motion and the boundary conditions. From the equations of motion, unknown variables are eliminated. Then the boundary conditions are used to eliminate further unknowns and finally a set of approximate boundary conditions remains. This has been performed for both one-dimensional and two-dimensional cases. The one-dimensional approximate boundary conditions have been developed both for a piezoelectric actuator and a piezoelectric sensor.

The one-dimensional piezoelectric actuator placed on an isotropic half-space is considered in the first numerical example. An elastic wave is induced in the half-space by applying a voltage difference to the piezoelectric layer. The second numerical example is the one-dimensional piezoelectric sensor which also is placed on an isotropic half-space. The difference between this case and the previous is that there is no applied voltage. Instead there is an incident wave in the half-space that is inducing a voltage jump in the piezoelectric layer. The third numerical example shows the dispersion curves obtained from using the two-dimensional approximate boundary conditions. Here, a thin piezoelectric layer with shorted electrodes is

perfectly bonded to an elastic plate. The dispersion curves are calculated for different thickness ratios of the piezoelectric layer and the elastic plate.

The numerical examples show the limitations of the approximate boundary conditions. It is shown that the first order approximate boundary condition is good at low frequencies and thin piezoelectric layers, i.e., thin compared to the wavelength in the layer. Since many industrial applications are concerned with thin piezoelectric layers and low frequencies, the lowest order approximate boundary conditions determined in this paper can be used to simplify the calculations greatly. At higher frequencies, the second and third order approximate boundary conditions work better. They are, however, more complicated which reduces the benefit in using them.

The greatest benefit of using these boundary conditions is that the system of equations that needs to be solved is smaller since the piezoelectric layer is completely eliminated and replaced by a set of boundary conditions. An interesting use of the approximate boundary conditions could be to implement them in FEM programs without the capability to handle piezoelectric materials.

Acknowledgement

The authors would like to thank Prof. Anders Boström for many valuable discussions.

References

Ammari, H., He, S., 1997. Generalized effective impedance boundary conditions for an inhomogeneous thin layer in electromagnetic scattering. J. Electromagn. Waves Appl. 11, 1197–1212.

Auld, B.A., 1990. Acoustic Fields and Waves in Solids, vols. 1 and 2. Krieger, Malabar, FL.

Batra, R.C., Liang, X.Q., Yang, J.S., 1996. The vibration of a simply supported rectangular elastic plate due to piezoelectric actuators. Int. J. Solids Struct. 33, 1597–1618.

Boström, A., Johansson, G., Olsson, P., 2001. On the rational derivation of a hierarchy of dynamic equations for a homogeneous, isotropic, elastic plate. Int. J. Solids Struct. 38, 2487–2501.

Bövik, P., 1994. On the modelling of thin interface layers in elastic and acoustic scattering problems. Quart. J. Mech. Appl. Math. 47, 17–42.

Gao, J.-X., Shen, Y.-P., Wang, J., 1998. Three dimensional analysis for free vibration of rectangular composite laminates with piezoelectric layers. J. Sound Vibrat. 213, 383–390.

Gopinathan, S.V., Varadan, V.V., Varadan, V.K., 2000. A review and critique of theories for piezoelectric laminates. Smart Mater. Struct. 9, 24–48.

Idemen, M., 1988. Straightforward derivation of boundary conditions on sheet simulating an anisotropic thin layer. Electron. Lett. 24 (11), 663–665.

Johansson, G., 1999. Dynamic equations for layered piezoelectric plates by power series expansions. Tech. Rep. 1999:1. Dept. Mechanics, Chalmers Univ. Tech., Göteborg, Sweden.

Kim, J., Varadan, V.V., Varadan, V.K., 1996. Finite element modeling of structures including piezoelectric active devices. Int. J. Num. Meth. Eng. 40, 1–16.

Niklasson, A.J., Datta, S.K., Dunn, M.L., 2000a. On approximating guided waves in plates with thin anisotropic coatings by means of effective boundary conditions. J. Acoust. Soc. Am. 108, 924–933.

Niklasson, A.J., Datta, S.K., Dunn, M.L., 2000b. On ultrasonic guided waves in a thin anisotropic layer lying between two isotropic layers. J. Acoust. Soc. Am. 108, 2005–2011.

Rokhlin, S.I., Huang, W., 1993. Ultrasonic wave interaction with a thin anisotropic layer between two anisotropic solids. II Second-order asymptotic boundary conditions. J. Acoust. Soc. Am. 94, 3405–3420.

Tiersten, H.F., 1969. Linear Piezoelectric Plate Vibrations. Plenum Press, New York, NY.

Tiersten, H.F., 1993. Electroelastic equations for electroded thin plates subjected to large driving voltages. J. Appl. Phys. 74, 3389–3393.

Tzou, H.S., 1993. Piezoelectric Shells. Kluwer Academic Publishers, Dordrecht, The Netherlands.

Wang, J., Yang, J., 2000. Higher-order theories of piezoelectric plates and applications. Appl. Mech. Rev. 53, 87–99.

Wolfram, S., 1999. The Mathematica Book, fourth ed. Cambridge University Press.